Article

Not peer-reviewed version

Fabrication of Graphene Oxide and Conductive Polymer on Cotton Fabric with Ultrasonic (US) Assisted Dyeing for Washable E-Textiles

Nazakat Ali Khoso *, Arsalan Ahmed Sheikh, Sanam Irum Memon, Raja Fahad Qureshi, Abdul Malik Rehan Abbasi, Syed Qutaba, JiaJun Wang *

Posted Date: 27 June 2024

doi: 10.20944/preprints202406.1920.v1

Keywords: Graphene, Graphene Oxide, reduced Graphene Oxide, Cold pad Dyeing, Wearable, E-textiles

Article

Fabrication of Graphene Oxide and Conductive Polymer on Cotton Fabric with Ultrasonic (US) Assisted Dyeing for Washable E-Textiles

Nazakat Ali Khoso [1,*], Arsalan Ahmed Sheikh [2] Sanam Irum Memon [3], Raja Fahad Qureshi [3], Abdul Malik Rehan Abbasi [1], Syed Qutiaba [1] and JiaJun Wang [4,*]

[1] Department of Textile Engineering and Design, FOE and Architecture, BUITEMS, Quetta Pakistan
[2] Department Textile Engineering and Clothing, NTU, Karachi Campus Sindh Pakistan
[3] Department of Textile Engineering, FOE, Mehran UET, Jamshoro Sindh Pakistan
[4] School of fashion and Desing, Zhejiang Sci-Tech University, Hangzhou, P.R China
* Correspondence: Nazakat.ali@buitms.edu.pk (N.A.K.); Wangjjhz@163.com (J.W.)

Abstract: The graphene based highly conductive and flexible devices has received momentous attraction and growth in recent years for potential multifunctional uses. The development of flexible and washable textile sensors, actuators, energy storage and energy harvesting systems. Textile fabrics coated with graphene and conductive polymers have been used for wearable self-powered e-textiles, such as tribo-electric, piezoelectric, and Thermoelectric. Herein this research, 100% woven cotton fabric is Fictionalized with graphene oxide (GO) using industrial-scale cold pad batch dyeing technique for the development of low-grade body heat into self-powered wearable e-textiles. The conductive polymer PEDOT: PSS was coated using layer by layer approach. The study demonstrates that the resultant textile electrodes showed reduced electrical sheet resistance from 2.5 MΩ to 15KΩ, with a reduced graphene oxide and further reduced to (2.5 -12.5 Ω) for conductive polymer. The sheet resistance was decreased with the number of dyeing cycles (10-15) and increased with 20 washing cycles vice versa. The study demonstrates that the sensor response and performance were improved with increasing the content percent of rGO and PEDOT: PSS. The tensile strength of as coated fabric electrodes was improved from (25.0-85.5 mPa) and fabric thickness was increased to (26-38μm) without compromising or influencing the air permeability. The resultant textile electrodes may potentially be used in smart textiles for self-powered flexible wearable generators, sensors, and energy storage. The study demonstrates that the cold pad batch dyeing method is a suitable and effective method for the fabrication of graphene-based textiles.

Keywords: graphene; graphene oxide; reduced graphene oxide; cold pad dyeing; wearable; e-textiles

1. Introduction

The demand for highly flexible and conductive textiles received great attention from the researchers and the scientific community to transfer the technology. The development of such highly flexible, conductive, and breathable textiles for smart clothing is under investigation.[1] There is still a sufficient gap in the growth of new materials and methods for the processing of such wearable devices embedded in e-textiles. In order to provide an alternative solution to new materials towards, process and product development is highly anticipated for sustainable energy harvesting and storage devices[2]. There is great significance of new materials, cost effective process, and green approaches towards the synthesis of appropriate in wearable devices for health monitoring and energy conversion.[2] Several materials such as metal oxides include silver (AgNP), copper (CuNP), and gold (AuNP) titanium dioxide (TiO_2), Bismuth Telluride,(Bi_2Te_3) and Selenium Telluride (Sn_2Te_3) with graphene have been used as reported in literature and previous studies.[3][4] Whereas, these metal-based compounds are limited to their use in textiles due to low stability, poor washing and skin irritation.[5] In this concern, the use of carbon-based materials such as graphite, graphene, graphene oxide, carbon nanotube, and reduced graphene oxide has been introduced for wearable sensors, and actuators for biomedical and health monitoring devices.[6]

 doi:10.20944/preprints202406.1920.v1

Graphene is considered as one of the new materials that has been used in the field of textile, material science and other related research fields.[7] The graphene is highly efficient and as well as some novel 2D material including boron nitrite (hBN), Phosphorous, and MXene has been recently used for the development of such highly flexible and wearable e-textiles.[8] These 2D materials has several attributes, such as outstanding optical,[9] electronic,[10] electrical,[11] thermal and mechanical behavior.[12] So; due to these exceptional properties these materials are being used for multi-functional finishing of textiles including water[13] and oil repellent,[14] flame proof,[15] fire retardant [16], antibacterial,[17] antiseptic, [18] UV-protection,[19] dust proof,[20] photo catalytic,[21] anti-static,[22] anti-corrosion,[23] EMI shielding,[24] self-cleaning[25] and self-healing[26] textiles without influencing breath ability of wearable textiles.[27] However, in this concern several fabrication techniques such as dip coating,[28] spin coating,[29] spray coating,[30] roll to roll printing,[31] pad dry cure,[32] exhaust dyeing,[33] screen printing,[34] digital ink jet printing,[35] and 3D printing [36] for the designing of wearable flexible devices. Among these known methods cold and batch process as Ultra sonication (US) dyeing is considered as highly efficient method for the fabrication of graphene to develop washable, and breathable conductive textile fabrics.[37-39] Graphene is rGO under material in the field of material since as well as textile engineering as Graphene coated textile garments are breathable, washable, flexible, stretchable, and comfortable to wearer.[40] Furthermore, the graphene dyed textile fabrics can also be used for energy storage, conversion, and harvesting systems.[41] These self-powered wearable e-textiles are such as Thermoelectric,[42] pyroelectric,[43] piezoelectric,[44] thermoelectric,[45] solar cells,[46] and super-capacitors for energy harvesting and storage.[47-48] without compromising the functional and aesthetic properties of textiles [49] for example breath ability,[50] bending,[51] stretching,[52] washing,[53] and cyclic loading[54] which allows better moisture transport and absorption of heat transport from body, and can be potentially used for green wearable TE devices.[55] Therefore, alternatively the use of highly conductive conjugated polymers been introduced to improve the electrical, and sensor performance with improved electrical conductivity and thermal conductivity.[56] These properties may tuned with the addition of dopants; such as fullerene, black carbon, CNT, graphite, graphene, and reduced rGO.[57-58] Herein, this research work we used a water based graphene oxide (GO) dye solution, contains carboxyl, hydroxyl, phenolic and epoxides groups; which improves the fixation and binding attributes of graphene oxide on the textile substrate as a dye as compared to insoluble carbon based materials and require some dispersing agents, binder and thickeners. The cold pad batch process is a production scale fabrication of textiles as compared to other commercially available techniques. This study provides the preparation of breathable graphene-coated 100% cotton fabric by using GO as a dye solution on the padder machine without using any binder and thickener as the state of the art of this research work.

2. Materials and Methods

The pure graphite powder with a particle size of 45 microns was obtained from Asbury USA, with 200 m^2/g surface area, >99% purity, and was fibre to Graphene oxide and reduced graphene oxide (rGO). The 100% woven fabric scoured and bleached cotton fabric with (250 GSM) supplied by the Hangzhou Bleaching and Dyeing Mills Pvt. Ltd, China. All the other chemicals and distilled water for the preparation of PEDOT: PSS-rGO as dye solutions were used for analytical grade without further modifications.

2.1. Synthesis of GO

Graphene Oxide (GO) was prepared using modified Hummer's method, as reported in the literature and our previous work.[59]

2.2. Fabrication of Graphene (Ultra sonication)

Initially, 250 ml of distilled water and 25 mL of PEDOT: PSS was added with different weight percent of as-synthesized rGO (0.5~2.5) gm/L powder and mixed ultrasonically for 30 min at RT to

 doi:10.20944/preprints202406.1920.v1

develop the rGO-PEDOT: PSS dye solution without using any dispersing agent and binder. After the aqueous dispersion of GO as a dye solution loaded ultra-sonication bath with fabric to liquor ratio of (1:40). During the dyeing process the fabric was loaded in ultra-sonication chamber with frequency of 250-300 MHz for 2-3 hours. The same procedure was repeated several times with variable Graphene oxide in water-based dye solution bath, until unless the significant coating of graphene oxide was obtained. After coating the dyed (GO) samples were Air dried at 60 °C for 10~20 min. Then dipped in L-Ascorbic Acid (20%) as reducing agent for the reduction of GO coated cotton fabric intro rGO at 90 °C for 2-3 hrs as reported previous studies.[62] Finally, the rGO coated fabric samples were microwave assisted cured at 145 °C for 3-4 min. Finally, wash with plenty of Deionized water to remove the acid traces and unfixed rGO flakes from the fiber surface.

2.3. Reduction (rGO)

The water-based GO solution was used as a dye solution after the fabrication of GOp-PES using the pad batch dyeing process. The fabric was dried at 60 °C and reduced into rGO using a green, reducing agent (L-Ascorbic Acid) over a reduction temperature of 90-100 C. followed by cured at 100~140 °C for 10~15 minutes. As reported in literature and in our previous works.[60]

2.4. Designing Wearable TE Device

The textile-based wearable sensor device was fabricated by cutting as coated rGO and PEDOT: PSS strips with size of (0.5x2.5 cm). The arrangement of device was made by connecting fabric strips using adhesive copper tape. The open-circuit voltage, change in resistance was measured using digital voltmeter connected with lab view software as reported previous studies.[61] The resultant sensory device was placed to human wrist to measure performance without any masking tape.

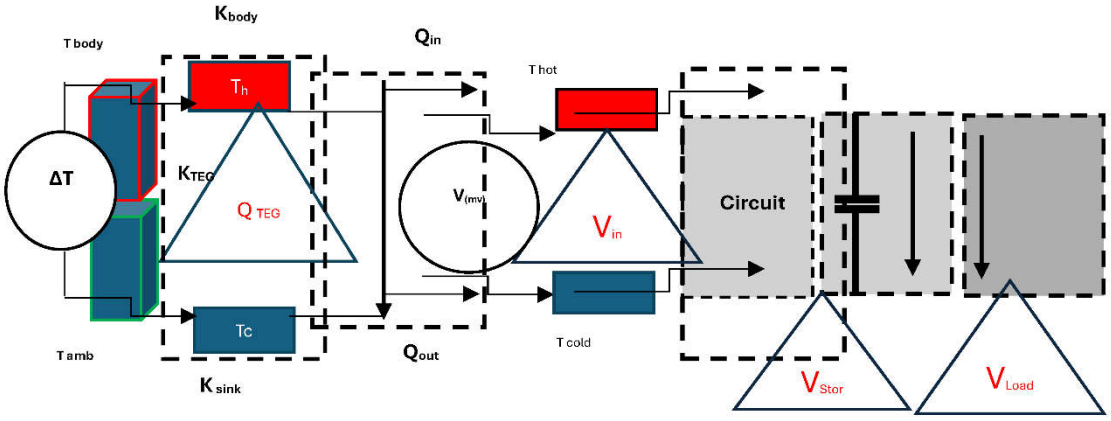

Figure 1. Fabrication of TE device with design model for wearable Nanogenerator circuit diagram with hot and cold sides of device connected to (Th) human body and (Tc) as cold side open to external environment.

3. Characterizations

Characterization for elemental analysis was performed using FTIR, XRD, Raman and XPS respectively. The surface characterization was made using SEM and EDX's analysis. The electrical performance for sheet resistance was measured using key sight and Keithley digital voltmeter according to ASTM standard D-257 [62] for polymer coated conductive textiles. The electrical performance of as coated fabric was measured before and after washing in terms of change in sheet resistance (Rs) of as coated textile electrodes with rGO, PEDOT: PSS, and rGO-PEDOT:PSS nanocomposites with variable weight of rGO. The statistical analysis was made by taking average values were recorded for each tested sample for sheet resistance of each sample were measured five times for statistical analysis. The electrical conductivity was measured from obtained results of sheet resistance. After washing and cleaning, the resultant rGO coated fabric was tested for electrical

 doi:10.20944/preprints202406.1920.v1

conductivity and thermal conductivity, sensor response using Key sight and digital voltmeters for each coated fabric.

3.1. FESEM

The surface characterization was made using field emission electron microscopy FESEM with elemental analysis supported software (EDS) analysis. The results are demonstrated in Figure 2 The SEM results show that, the entire fiber surface is coated with smooth layer of graphene and fiber-fiber bonding with strong interaction between rGO films and conductive polymer as compared to pristine fabric demonstrated in Figure 2 a) b) & c) respectively. The presence of carbon, oxygen and sulphone groups can be depicted from elemental (EDS) analysis.

The results show that the rGO coated fiber surface with bonding between graphene and polymer films, introducing conductive fiber paths due to the strong adhesion of conductive polymers. The fibre surface in the yarn was entirely covered with PEDOT: PSS and rGO due to the strong adhesion and bonding of the available conjugated polymer. The fibre surface was covered with smooth coating of rGO as the number of dyeing cycles increased. Followed by a coating of the PEDOT: PSS with 5-10µm size increased as compared to undercoated samples. Figure 2 d) e) & f) demonstrates the elemental (EDs) analysis of rGO and conductive polymer coated fabric with colored mapping of each element carbon (C), oxygen (O) and sulfur groups respectively by using FESEM. Which, clearly shows that fibre surface is covered with smooth layers of rGO and PEDOT: PSS films.[63]

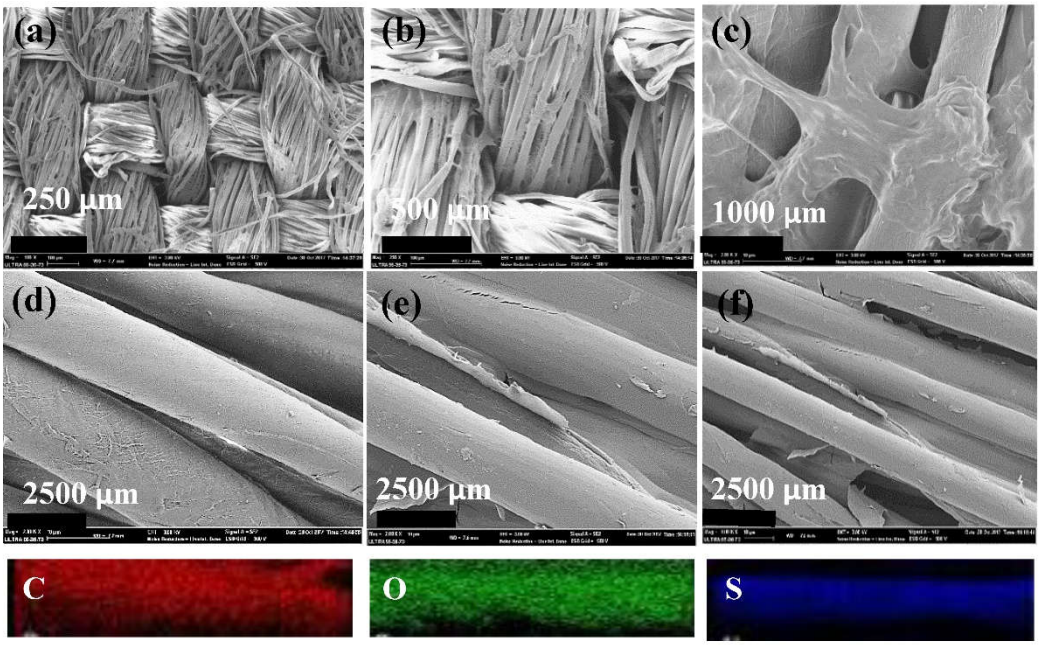

Figure 2. SEM image of a) GO, rGO and rGO-PEDOT: PSS Coated Fabric with different magnifications b) Color Mapping for elemental analysis using (EDS) with SEM images [Reproduced with Copyright Materials, RSC Advances, Royal Society of Chemistry, 2021.[64].

3.2. XRD Analysis

The elemental analysis of the as coated rGO fabric was performed using XRD to identify the crystalline regions of rGO and PEDOT: PSS respectively. The X-ray Diffraction results showed that, firm peaks for GO 2θ located at 10.0°-12.0°. The crystallize and amorphous regions of textile cotton fabric was made using XRD diffraction over a range of degree 2(theta) of 20-80 and scan rate of 5° deg/minute. The diffraction results confirm the broader peaks for GO coated fabric over 9.5°, which is gradually shifted towards 16.5-22.5° and reduced the height of the broader peaks when reduced into rGO after chemical and thermal reduction as compared to GO and pristine graphite. The newly developed broader peaks show the extending and widening of rGO films after reduction. On the other hand, these peaks are assigned to re stacking of GO films into larger in crystal size.[65] The

 doi:10.20944/preprints202406.1920.v1

similar broader and widened smaller peaks has been observed at 34.5° which may be attributed to conductive polymer with formation of crystal and formation of flakes. The results showed that graphene oxide was successfully converted into reduced graphene oxides, as shown in the Figure 3 a) & b) as compared to the sharp XRD peaks of pristine graphite at 28.4° have been reduced when graphitic oxide was converted into GO and further reduced to 22.5° for rGO. The second small peak observed at 34.6°, this diffraction peak may be attributed to crystal formation of PEDOT: PSS. The peaks with d-spacing of 0.85nm and d-spacing of d = 0.346 to d = 0.353 with crystal planes (001), (010) and (002) as reduced to rGO as compared to pristine graphite with d-spacing of d=0.339 nm as shown in Figure 3 c) & d) respectively.[66]

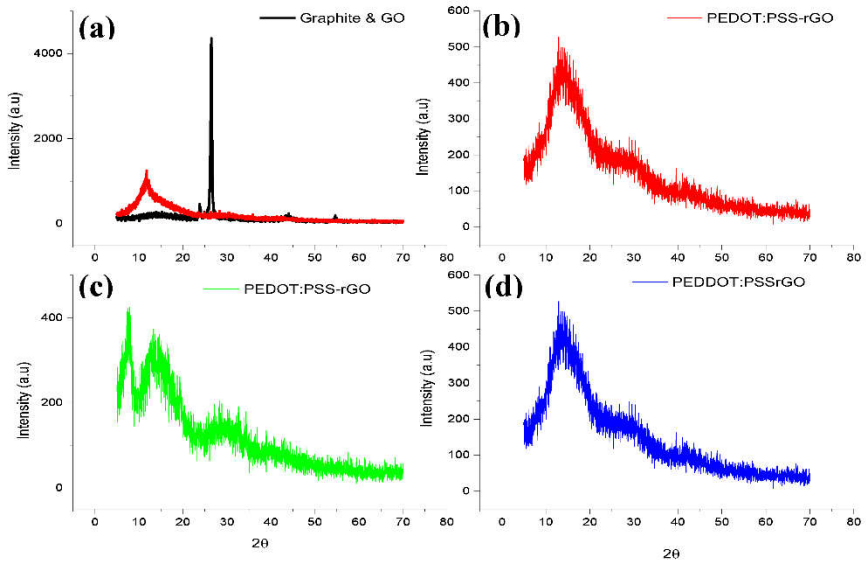

Figure 3. a) XRD analysis of pure graphite and GO a) PEDOT:PSS-rGO with variable content percent of rGO in conductive polymer 2.5 b), 5.0 c) and 10.0d).

3.3. Raman Analysis

The Raman Spectra shows identical peaks (D and G-bands), demonstrating the highly oxidized two-dimensional hexagonal structures of carbon atoms. The Raman spectroscopy analysis was performed to identify the oxidization and crystallization of Sp^3 to Sp^2 hybridization of carbon atoms during synthesis of GO and after reduction. The Raman spectra show that, the opening of graphitic films into highly exfoliated Graphitic oxide using strong acids and oxidizing agents.[67] The two identical peaks (I_D) and (I_G) were found to be more widened with (I_D/I_G) ratio of 0.85, 0.90 which increased when oxidized and reduced (G) bands when oxygen groups were eliminated and removed after thermal and chemical annealing. These two broader and widened peaks are allocated to graphene oxide with first order to second order (D &G) vibrational peaks positioned at 1355 Cm^{-1} and 1583 Cm^{-1}, which may attributed to reduction of oxygen-containing functional groups as compared to GO with 1560 Cm^{-1} as shown in Figure 4 a & b)[68] Whereas, the vibrational small dangling bands are occurred between D and G bands, which are attribute to thiophene and sulphone groups present in conductive polymer. These changes are attributed to hybridization of carbon atoms after addiction of conductive polymers, which may decrease the oxygen functional group after the reduction of GO into rGO. The results also demonstrate that graphene oxide is oxidized state changed from the first-order scattering of SP^3 to Sp^2 hybridization. The re-stacking of carbon atoms in the case of rGO during chemical and thermal annealing with different weight percent of rGO and reducing agent L-Ascorbic Acid as shown in Figure 4 c) & d). Whereas the dangling bands occurred between the D and G-bands of rGO, may attributed to the presence of sulphone groups present in PEDOT: PSS films.

 doi:10.20944/preprints202406.1920.v1

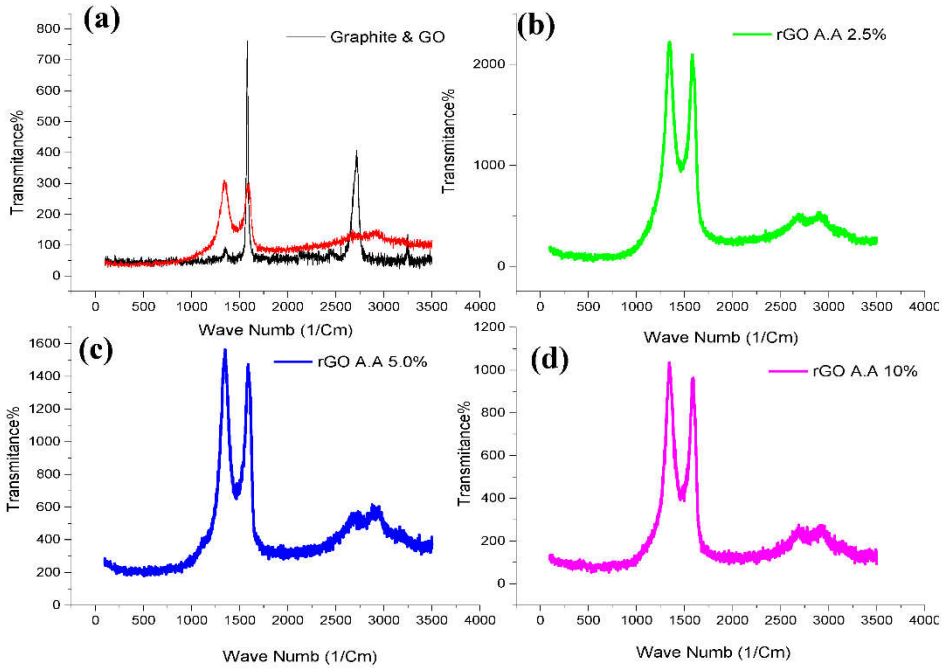

Figure 4. Raman Spectroscopy of pure graphite & GO a) rGO with different reduction of L-Ascorbic Acid b), c) & d) .

3.4. FTIR Analysis

The FTIR/ATR analysis of as coated fabric with GO, rGO, and PEDOT: PSS shows several functional moieties and reactive functional groups available in GO including water traces such as (OH) hydroxyl groups positioned at 3400 cm^{-1}. Whereas other functional groups present in rGO and PEDOT: PSS nanocomposite are positioned at 1250, 1365, 1650 cm^{-1} are assigned to sulphone, groups as compared to pristine GO and rGO. Whereas, on the other hand, the broader and wider spectral and several sharp peaks are positioned at 3450 cm-1, 1350, 1425 and 1665 cm^{-1}. Whereas this hydroxyl broader and widened peaks have been diminished and reduced for rGO as compared to GO and PEDOT:PSS coated textile substrate. The availability and presence of new reactive functional groups are allocated and slightly shifted towards at 1355 cm^{-1}, 1668 cm^{-1} and 1735 cm^{-1}; which shows that the PEDOT:PSS entirely covered the newly development chemical shifts. Similarly, the d-convoluted reactive groups are assigned to the vibrational of absorption of water molecules hydroxyl (OH^{-}) (3400 cm^{-1}), carbonyl C=O (1740 cm^{-1}), carbonyl (C-C-) deformation peak (1420 cm-1), carboxyl (C=C) (1220 cm^{-1}), Carboxyl C-O (1650 cm^{-1}) and epoxy 1620 cm^{-1} respectively.[69]

4. Textile Properties

All the tests were performed according to standard humidity 65±2 and temperature of 25±5 ºC according to ASTM standard [70]. The test results were recorded manually, and each sample was measured five times. The average test results were calculated from obtained results with standard deviation.

4.1. Air Permeability

The air permeability of the coated samples of GO, rGO, and PEDOT: PSS-rGO was analyzed according to ASTM standards D-737-18.[56] Each sample was studied before dyeing and the number of washing cycles to measure the breath ability of the as coated textile substrates. The breathing properties before and after coating with GO, rGO and PEDOT:PSS nanocomposite was analyzed using ASTM standard D-737-18.[71] The air penetrability before and after washing of each coated sample was measured using automatic air permeability tester. The results demonstrates that, the air permeability, and washing stability are directly proportional to the number of dyeing cycles with

 doi:10.20944/preprints202406.1920.v1

improved electrical conductivity, which may result due to improved conductive channels and less air gaps as number of dyeing cycles were increased. The properties were significantly reduced after number of washing cycles, which may occur due to the removal of graphene films from the fiber surface as well as between fiber gaps. These gaps are mostly filled with rGO films and conductive polymer in which PSS worked as binder. The results also reveal that the air permeability of undercoated samples was decreased as the number of dyeing cycles. Whereas the air permeability was slightly influenced as the opened fiber assembly become more compact after coating of rGO layers as smooth coating. The sheet resistance and permeability were decreased as the number of dyeing cycles increased; with improved number of layers of rGO and PEDOT: PSS. PEDOT as compared to pristine GO and rGO coatings. The resultant fabric properties are substantial for breathable; wearable and washable without influencing the breath ability in terms of comfort properties without compromising the moisture and air transport.

4.2. Water Contact Angle (WCA)

The water absorption properties were measured using a water contact angle device, according to ASTM standard D-5725. The hydrophobic and hydrophilic attributes of the substrate before and after the coating were analyzed digital contact angle analyzer. The DI water was used to measure the contact angle of the as GO, rGO and rGO-PEDOT:PSS coated textile fabric [72] The study results reveal that, the hydrophobic nature of the fabric was improved with increasing the number of dyeing cycles and reduced with number of washing cycles. The maximum water contact angle of 131° and 142° was obtained with 10 ~15 number of padding passes as presented in Figure 5 c).

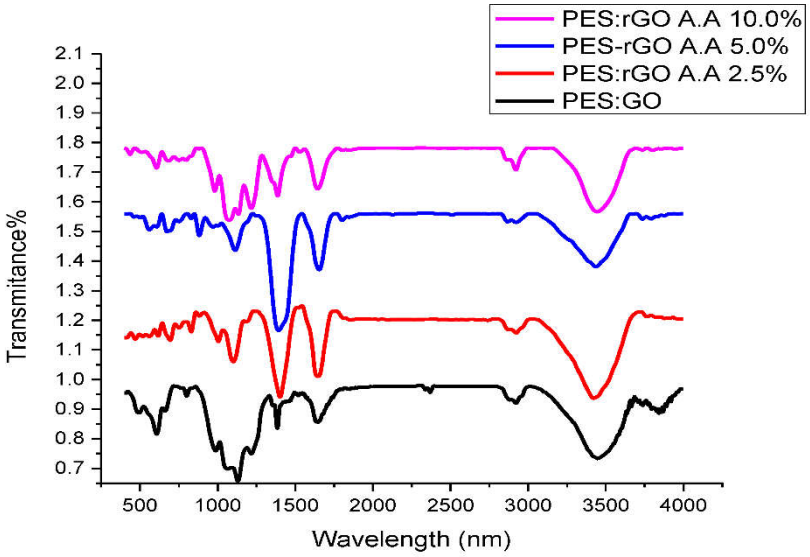

Figure 5. FTIR analysis of pure GO and PEDOT:PSS and variable content percent of rGO and reducing agent.

Furthermore, it is revealed from the results, that the rGO coated textile fabric showed higher water resistance and lowered the wettability as compared untreated cotton fabric and GO coated fabric sample. The performance results: it was observed that the rGO and PEDOT:PSS coated samples with different weight percent of rGO in the conductive polymer showed improved WCA as compared to pristine cotton fabric and GO coated fabric. The water droplet immediately disappears water droplet disappears and seeps out into the fabric in 1-2 seconds. For pure cotton and GO coated, as hydrophilic behavior and remain stable on surface of fabric for rGO coated substrate which shows hydrophobic attribute of the resultant fabrics. The results are presented in Figure 5 c) and demonstrated in Table 1 are in strong agreement with previously reported studies on rGO coated cotton fabrics.

 doi:10.20944/preprints202406.1920.v1

Table 1. Effect of different weight percent of rGO and PEDOT: PSS on tensile strength and Air permeability.

Sample details	Dyeing Cycles (KΩ)	Washing Cycles (KΩ)	Fabric Thickness (mm)	Tensile Strength (mPa)	Water Contact Angle (WCA)	Air Permeability (g/Cm²/S)
Pure Cotton			22	10	6-12	76
GO			25	12	20	74
rGO	185	195	26	20	45	72
P-rGO-1	145	150	27	40	70	69
P-rGO-2	125	135	28	60	84	66
P-rGO-3	115	125	29	75	96	63
P-rGO-4	85	95	30	80	110	60
Pure Cotton	185	195	26	20	45	72

4.3. Tensile Strength

The tensile strength of the as coated with rGO, and PEDOT:PSS-rGO fabric was performed using ASTM standard D-5035-11. [58] The tensile properties of textile fabric were made before coating and after coating. The results demonstrate in Figure 5 d) shows that the mechanical strength was increased warp and weft wise respectively. The tensile strength in terms of mechanical performance of as coated textile cotton fabric was improved with number of padding passes, results in improved graphene layers which improved tensile strength and stress of the resultant fabric as compared to untreated fabric samples.

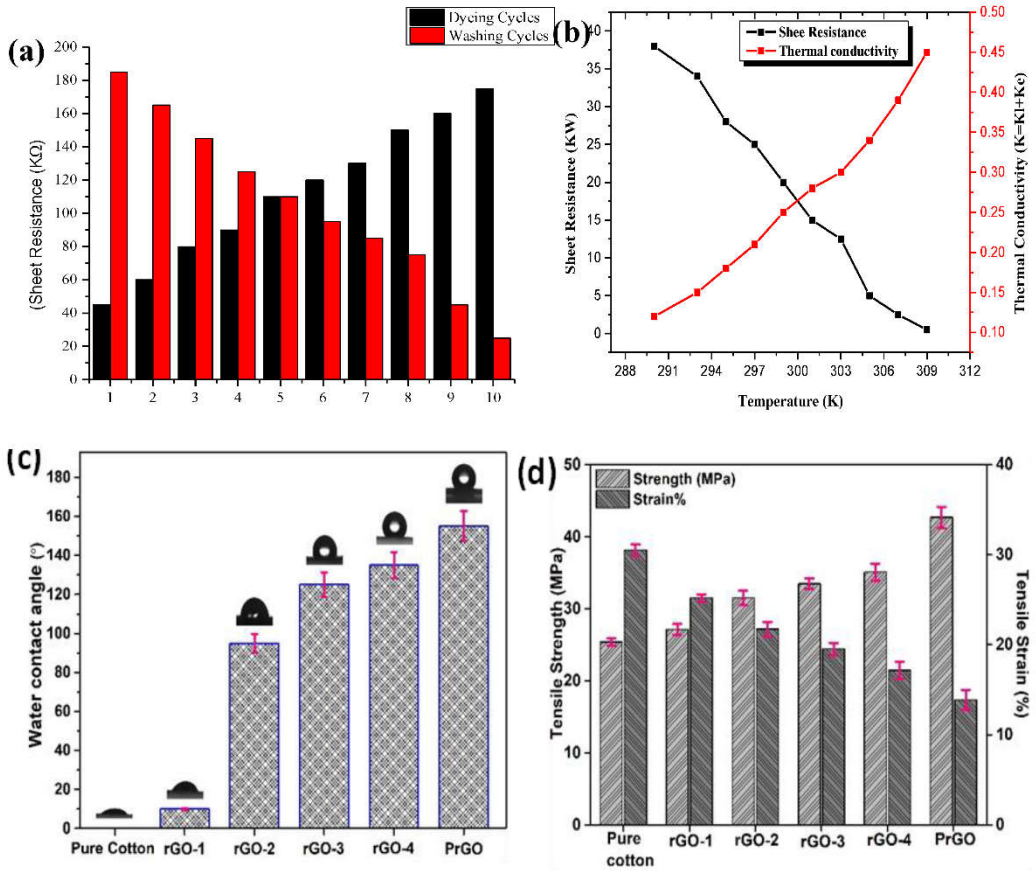

Figure 6. Performance analysis of coated textile substrate against number of dyeing and washing cycles a) Change in Sheet Resistance and thermal conductivity b) Water contact Angle c) Tensile Strength in (MPa) of pure cotton fabric and coated with different weight percent of rGO d).

 doi:10.20944/preprints202406.1920.v1

The results shows that the tensile strength was much higher on warp wise as compared weft wise direction, which may attribute to a greater number of ends as compared to picks in the fabric structure, and weft wise, with low yarn twist; which lead more pick up of GO and PEDOT:PSS-rGO on the fiber surface. The tests were performed with scan rate of 20mm/minutes. The results are presented in Table 2, which indicates that the strength was improved from 10-60 and 20-80 mPa weft and warp wise respectively as shown in Figure 5 b). Furthermore, the rGO content percent was increased to 20% resulted as highest tensile strength of 80mPa as compared untreated GO coated textile fibers. The results demonstrate that as the concentration of rGO was increased, it improved in tensile strength of the as coated textile fabric. As, the conductive polymer PEDOT: PSS Nano films entirely covered the fibrous yarn structure surface with rGO sheets, which may occur due to the reinforcement of the PSS and improved the tensile the overall textile properties.[73]

Table 2. Fabric thickness after several coating and its effect on electrical and thermoelectric properties.

Sample No.	Composition (GO-PES%)	Average thickness (mm)	Electrical Conductivity (KΩ)		
			Before Washing	After Washing	Bending Cycles
Untreated	Nil	22.0			
GO		25.0	95.2	5.0	10.0
P-rGO-1	2.5	26.5	88.6	12.5	15.5
P-rGO-2	5.0	27.7	74.8	18.5	22.5
P-rGO-3	7.5	28.5	62.5	25.0	28.5
P-rGO-4	10.0	30.4	31.9	35.6	38.5

5. Performance Measurements

5.1. Electrical Performance (Sheet Resistance)

The overall electrical performance in terms of sheet resistance of resultant textile electrode coated with rGO and PEDO: PSS was decreased from 185 KΩ to 45 KΩ with increasing the number of dyeing cycles; is attributed to more graphene layers on the fiber surface and development of conductive paths with strong bonding and adhesion. The sheet resistance was further decreased with coating with conductive polymer, resulting in the sheet resistance of 45-15KΩ; which can be seen in FESM results as demonstrated in Figure 5 a). Whereas on another, the sheet resistance was adversely influenced by increasing the number of washing cycles; which may be attributed to removal of graphene layers and unfixed graphene films between fibrous assembly.[74] The results also show that; the electrical sheet resistance was decreased from 85KΩ to 10~15Ω, when conductive polymer was coated on as rGO coated fabric. This synergetic effect is attributed to the higher interaction and bonding of fiber channels with graphene layers and PEDOT:PSS; which may improve with increasing padding passes introducing more conductive fibre-fiber surface junctions.

5.2. Thermoelectric Performance

Thermoelectric performance in terms of power factor, Seebeck coefficient and output voltages of the wearable TE device was measured using ASTM standard E-977-05[75]. The thermal gradient was measured using a hot plate based Seebeck setup and 2-probe thermocouples connected with digital voltmeter over a variable temperature of 20 °C-36.5 °C. The thermal conductivity and diffusivity of the developed textile-based TE device was measured using Infra-Red (IR)-noncontact device, according to ASTM standard D-7984-16 [76].

The results show that heat retention may result as the vibration movement of heat carrying phonon lateral transport instead of linear transport. The synergetic effect may occur due to the number of Graphene layers resulting in an enhanced electrical conductivity with more inter-junction of Graphene films and conductive polymer on the fiber surface with higher conductive paths. As a result, the thermoelectric performance was increased in terms of Seebeck coefficient, power factor

 doi:10.20944/preprints202406.1920.v1

and output electric potential. The thermoelectric effect was measured over the thermal gradient between the human body heat and external environmental temperature. The obtained results presented in Table 2 and Figure 6 g) which clearly demonstrate that, the TE effect of the as coated textile electrode improved the output open electric potential (ΔV) due to thermal difference between two types of materials (p-type) and heat flow in the rGO as p-type material at hetero-junctions of the TE device in the nanocomposite material.

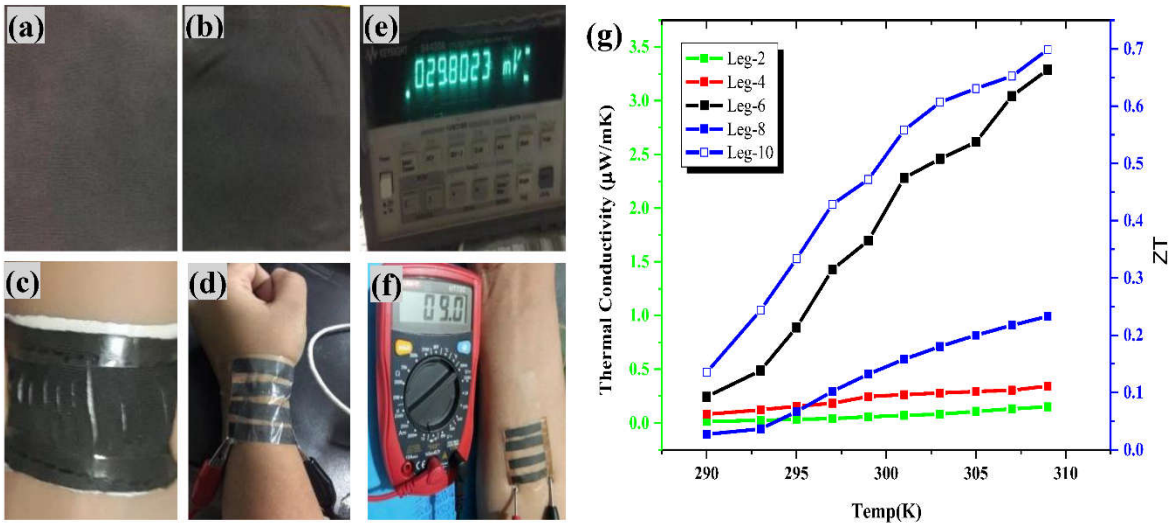

Figure 7. Fabrication of rGO coated fabric a) and Conductive polymer with rGO b) TE performance of Textile based (TEG) placed on back of the wrist c) & d) connected with Keysight and digital voltmeter e) & f) over all TE performance with number of TE legs shows Figure of Merit (ZT) value with change in temperature g).

The performance of TE device was measured over a temperature difference of 36.5 °C and an ambient temperature of (20°C), in which the thermal gradient (ΔT) of ±16.5 °C(309K). The temperature difference resulted as an electric potential (power) of 2.5~19.5mV for 2-Thermoelectric legs. As the TE legs were increased to 4-10 legs the output potential was improved from 20.0 mV to 70 mV for parallel and maximum reached to 120 mV in series arrangements; as shown in Figure 5 c) & d) respectively. The as coated with rGO and PEDOT: PSS respectively, the device was directly placed to human wrist. The overall thermoelectric performance of TE device is several orders of magnitude higher as compared to previously reported textile devices.[63] The developed TE device showed a Seebeck coefficient (25~65.0 μV/K), power factor (2.5~75μW/m^{-1}K^{2}), and dimensionless figure of merit (0.02~0.08x10^{-4}). The device was attached directly to human wrist and hand as shown in Figure 5 e) & f) respectively and Table 2.

The results demonstrate that, the thermoelectric dimensionless figure of merit, Seebeck coefficient, and power factor are enhanced with change in thermal gradient as function of temperature altered from 20~36.5 °C between the cold side and 20.0 to 36.5 °C hot side. The study reveals that the developed fabric is capable to directly convert the temperature difference into electric potential, and designed TE Nanogenerator can potentially be used for the conversion of human body heat into electrical energy. The resultant highly flexible, stretchable, and washable TE device with improved thermoelectric performance can be used instead of metal based rigid self-powered electronic devices for biomedical and health monitoring.[77]

6. Conclusions

In conclusion, the Graphene based highly flexible, stretchable and washable textile device is highly stable and capable of converting the human body heat as low-grade energy into electrical energy. The fabrication of graphene was accomplished successfully using cold pad batch dyeing technique, as an efficient and cost-effective method for the fabrication of graphene and conductive

 doi:10.20944/preprints202406.1920.v1

polymers. The results demonstrate that the electrical conductivity was improved in terms of sheet resistance with increasing the number of padding passes and reduced with number of washing cycles vice versa. The textile properties including air permeability, tensile strength and water contact angle were also improved increasing the content percent of rGO and number of padding passes. The resultant textile-based TE device showed improved thermoelectric performance in terms of Seebeck coefficient, power factor, and dimension less figure of merit (ZT) value from ($0.02\sim0.08\times10^{-4}$) as compared to pristine rGO and PEDOT: PSS coated textile fabrics. The Graphene coated textile fabric showed enhanced mechanical performance with tensile strength of 80 MPa, as well as enhanced water contact angle from (131°~141°) as compared to pristine cotton fabric and GO coated fabric. The PEDOT: PSS-rGO nanocomposite coated textile substrate showed higher performance without compromising the air permeability, washing stability and breathability. The resultant fabric is stable against 20 washing under rubbing fastness (wet and dry) conditions. The resultant textile fabric, coated with nanocomposite with better performance as compared to barely used rGO, while PEDOT:PSS with better fixation of graphene and enhanced washing fastness, tensile strength as well as thermoelectric performance as compared to pristine cotton and coated with rGO. The proposed approach may potentially be used for the development of different textile fabrics for coating of graphene, graphene oxide, and rGO with conductive conjugated polymers for self-powered wearable electronics, energy storage, and conversion devices in biomedical and health monitoring.

Author Contributions: All the authors contributed equally in writeup, editing, drafting of the manuscript.

Funding: The APC was not funded by any institution and organization, which is paid by authors equal contribution.

Acknowledgments: There is no financial support obtained by the authors from any source.

Conflicts of Interest: The authors declare no conflicts of interest.

References

1. Kim, H., & Ahn, J. H. (2017). Graphene for flexible and wearable device applications. *Carbon*, *120*, 244-257.
2. Hu, L., Pasta, M., La Mantia, F., Cui, L., Jeong, S., Deshazer, H. D., & Cui, Y. (2010). Stretchable, porous, and conductive energy textiles. *Nano letters*, *10*(2), 708-714.
3. Aboutalebi, S. H., Jalili, R., Esrafilzadeh, D., Salari, M., Gholamvand, Z., Aminorroaya Yamini, S., & Innis, P. C. (2014). High-performance multifunctional graphene yarns: toward wearable all-carbon energy storage textiles. *ACS nano*, *8*(3), 2456-2466.
4. Acar, G., Ozturk, O., Golparvar, A. J., Elboshra, T. A., Böhringer, K., & Yapici, M. K. (2019). Wearable and flexible textile electrodes for biopotential signal monitoring: A review. *Electronics*, *8*(5), 479.
5. Kaushik, V., Lee, J., Hong, J., Lee, S., Lee, S., Seo, J., & Lee, T. (2015). Textile-based electronic components for energy applications: principles, problems, and perspective. *Nanomaterials*, *5*(3), 1493-1531.
6. Weng, W., Chen, P., He, S., Sun, X., & Peng, H. (2016). Smart electronic textiles. *Angewandte Chemie International Edition*, *55*(21), 6140-6169.
7. Wang, B., & Facchetti, A. (2019). Mechanically Flexible Conductors for Stretchable and Wearable E-Skin and E-Textile Devices. *Advanced Materials*, *31*(28), 1901408.
8. Novoselov, K. S., Fal, V. I., Colombo, L., Gellert, P. R., Schwab, M. G., & Kim, K. (2012). A roadmap for graphene. *Nature*, *490*(7419), 192-200.
9. Lee, D., Lee, H., Ahn, Y., Jeong, Y., Lee, D. Y., & Lee, Y. (2013). Highly stable and flexible silver nanowire–graphene hybrid transparent conducting electrodes for emerging optoelectronic devices. *Nanoscale*, *5*(17), 7750-7755.
10. Mirjalili, M. (2016). Preparation of electroconductive, magnetic, antibacterial, and ultraviolet-blocking cotton fabric using reduced graphene oxide nanosheets and magnetite nanoparticles. *Fibers and Polymers*, *17*(10), 1579-1588.
11. Zhang, Y., Xu, Q., Fu, F., & Liu, X. (2016). Durable antimicrobial cotton textiles modified with inorganic nanoparticles. *Cellulose*, *23*(5), 2791-2808.
12. Tissera, N. D., Wijesena, R. N., Perera, J. R., de Silva, K. N., & Amaratunge, G. A. (2015). Hydrophobic cotton textile surfaces using an amphiphilic graphene oxide (GO) coating. *Applied Surface Science*, *324*, 455-463.
13. Ji, Y., Li, Y., Chen, G., & Xing, T. (2017). Fire-resistant and highly electrically conductive silk fabrics fabricated with reduced graphene oxide via dry coating. *Materials & design*, *133*, 528-535.

 doi:10.20944/preprints202406.1920.v1

14. Karimi, L., Zohoori, S., & Amini, A. (2014). Multi-wall carbon nanotubes and nano titanium dioxide coated on cotton fabric for superior self-cleaning and UV blocking. *New Carbon Materials*, *29*(5), 380-385.
15. Chakraborty, J. N., Mohapatra, M. R., & Kumar, J. (2018). Differential functional finishes for textiles using graphene oxide. *Research Journal of Textile and Apparel*.
16. Montazer, M., & Seifollahzadeh, S. (2011). Enhanced self-cleaning, antibacterial and UV protection properties of nano TiO2 treated textile through enzymatic pretreatment. *Photochemistry and photobiology*, *87*(4), 877-883.
17. Madan, D., Chen, A., Wright, P. K., & Evans, J. W. (2012). Printed Se-doped MA n-type Bi 2 Te 3 thick-film thermoelectric generators. *Journal of electronic materials*, *41*(6), 1481-1486.
18. Madan, D., Wang, Z., Wright, P. K., & Evans, J. W. (2015). Printed flexible thermoelectric generators for use on low levels of waste heat. *Applied energy*, *156*, 587-592.
19. Abu-Thabit, N. Y., & Makhlouf, A. S. H. (2016). Smart Textile Supercapacitors Coated with Conducting Polymers for Energy Storage Applications. In *Industrial Applications for Intelligent Polymers and Coatings* (pp. 437-477). Springer, Cham.
20. Jia, L. C., Ding, K. Q., Ma, R. J., Wang, H. L., Sun, W. J., Yan, D. X., ... & Li, Z. M. (2019). Highly Conductive and Machine-Washable Textiles for Efficient Electromagnetic Interference Shielding. *Advanced Materials Technologies*, *4*(2), 1800503.
21. Liu, L., Yu, Y., Yan, C., Li, K., & Zheng, Z. (2015). Wearable energy-dense and power-dense supercapacitor yarns enabled by scalable graphene–metallic textile composite electrodes. *Nature communications*, *6*(1), 1-9.
22. Karimi, L., Zohoori, S., & Amini, A. (2014). Multi-wall carbon nanotubes and nano titanium dioxide coated on cotton fabric for superior self-cleaning and UV blocking. *New Carbon Materials*, *29*(5), 380-385.
23. Carey, T., Cacovich, S., Divitini, G., Ren, J., Mansouri, A., Kim, J. M., & Torrisi, F. (2017). Fully inkjet-printed two-dimensional material field-effect heterojunctions for wearable and textile electronics. *Nature communications*, *8*(1), 1-11.
24. Shao, Y., El-Kady, M. F., Wang, L. J., Zhang, Q., Li, Y., Wang, H., & Kaner, R. B. (2015). Graphene-based materials for flexible supercapacitors. *Chemical Society Reviews*, *44*(11), 3639-3665.
25. Montgomery, D. S., & Carroll, D. L. (2016). Improving upon flexible thin film thermoelectric generator design. *Coupled thermoelectric and piezoelectric Meta structures for renewable energy generation*, *96*, 56.
26. Navone, C., Soulier, M., Plissonnier, M., & Seiler, A. L. (2010). Development of (Bi, Sb) 2 (Te, Se) 3-based thermoelectric modules by a screen-printing process. *Journal of electronic materials*, *39*(9), 1755-1759.
27. Shathi, M. A., Minzhi, C., Khoso, N. A., Deb, H., Ahmed, A., & Sai, W. S. (2020). All organic graphene oxide and Poly (3, 4-ethylene dioxythiophene)-Poly (styrene sulfonate) coated knitted textile fabrics for wearable electrocardiography (ECG) monitoring. *Synthetic Metals*, *263*, 116329.
28. Sun, T., Wang, J. J., Khoso, N. A., Yu, L., & Zhang, Y. (2017). Facile synthesis of Poly (3, 4-ethylenedioxythiophene) nanostructure with controlled morphologies by using an aqueous surfactant soft-template-assisted technique. *Materials Letters*, *191*, 61-64.
29. Sun, Y. C. (2015). Development and Characterization of Next Generation Flexible Dielectric and Thermoelectric Energy Harvesting Materials (Doctoral dissertation).
30. Thielen, M., Sigrist, L., Magno, M., Hierold, C., & Benini, L. (2017). Human body heat for powering wearable devices: From thermal energy to application. *Energy conversion and management*, *131*, 44-54.
31. Tian, M., Hu, X., Qu, L., Du, M., Zhu, S., Sun, Y., & Han, G. (2016). Ultraviolet protection cotton fabric achieved via layer-by-layer self-assembly of graphene oxide and chitosan. *Applied Surface Science*, *377*, 141-148.
32. Tian, M., Hu, X., Qu, L., Zhu, S., Sun, Y., & Han, G. (2016). Versatile and ductile cotton fabric achieved via layer-by-layer self-assembly by consecutive adsorption of graphene doped PEDOT: PSS and chitosan. *Carbon*, *96*, 1166-1174.
33. Vondrak, J., Schmidt, M., Proto, A., Penhaker, M., Jargus, J., & Peter, L. (2019, June). Using Miniature Thermoelectric Generators for Wearable Energy Harvesting. In *2019 4th International Conference on Smart and Sustainable Technologies (SpliTech)* (pp. 1-6). IEEE.
34. Zeng, W., Shu, L., Li, Q., Chen, S., Wang, F., & Tao, X. M. (2014). Fiber-based wearable electronics: a review of materials, fabrication, devices, and applications. *Advanced materials*, *26*(31), 5310-5336.
35. Wong, H. P., & Dahari, Z. (2015, October). Human body parts heat energy harvesting using thermoelectric module. In *2015 IEEE Conference on Energy Conversion (CENCON)* (pp. 211-214). IEEE.
36. Hamada, J., Yamamoto, K., & Takashiri, M. (2018, July). Fabrication and characterization of roll-type thin-film thermoelectric generators. In *Journal of Physics: Conference Series* (Vol. 1052, No. 1, p. 012129). IOP Publishing.
37. Zhu, Z., Liu, C., Jiang, Q., Shi, H., Xu, J., Jiang, F., & Liu, E. (2015). Green DES mixture as a surface treatment recipe for improving the thermoelectric properties of PEDOT: PSS films. *Synthetic Metals*, *209*, 313-318.

 doi:10.20944/preprints202406.1920.v1

38. Dong, L., Xu, C., Li, Y., Wu, C., Jiang, B., Yang, Q., & Yang, Q. H. (2016). Simultaneous Production of High-Performance Flexible Textile Electrodes and Fiber Electrodes for Wearable Energy Storage. *Advanced Materials*, *28*(8), 1675-1681.
39. Du, Y., Xu, J., Wang, Y., & Lin, T. (2017). Thermoelectric properties of graphite-PEDOT: PSS coated flexible polyester fabrics. *Journal of Materials Science: Materials in Electronics*, *28*(8), 5796-5801.
40. Dunham, M. T., Barako, M. T., Cornett, J. E., Gao, Y., Haidar, S., Sun, N., & Goodson, K. E. (2018). Experimental characterization of microfabricated thermoelectric energy harvesters for smart sensor and wearable applications. *Advanced Materials Technologies*, *3*(6), 1700383.
41. Huang, Y., Hu, H., Huang, Y., Zhu, M., Meng, W., Liu, C., & Zhi, C. (2015). From industrially Weavable and knittable highly conductive yarns to large wearable energy storage textiles. *ACS nano*, *9*(5), 4766-4775.
42. Hyland, M., Hunter, H., Liu, J., Veety, E., & Vashaee, D. (2016). Wearable thermoelectric generators for human body heat harvesting. *Applied Energy*, *182*, 518-524.
43. Islam, M. Z., Dong, Y., Khoso, N. A., Ahmed, A., Deb, H., Zhu, Y., ... & Fu, Y. (2019). Continuous dyeing of graphene on cotton fabric: Binder-free approach for electromagnetic shielding. *Applied Surface Science*, *496*, 143636.
44. Jung, Y. S., Jeong, D. H., Kang, S. B., Kim, F., Jeong, M. H., Lee, K. S., ... & Choi, K. J. (2017). Wearable solar thermoelectric generator driven by unprecedentedly high temperature difference. *Nano energy*, *40*, 663-672.
45. Karim, N., Afroj, S., Tan, S., He, P., Fernando, A., Carr, C., & Novoselov, K. S. (2017). Scalable production of graphene-based wearable e-textiles. *ACS nano*, *11*(12), 12266-12275.
46. Pu, X., Liu, M., Li, L., Han, S., Li, X., Jiang, C., ... & Wang, Z. L. (2016). Wearable textile-based in-plane microsupercapacitors. *Advanced Energy Materials*, *6*(24), 1601254.
47. Sahito, I. A., & Khatri, A. (2017). Smart and Electronic Textiles. In *Advanced Textile Testing Techniques* (pp. 309-328). CRC Press.
48. Sahito, I. A., Sun, K. C., Arbab, A. A., Qadir, M. B., & Jeong, S. H. (2015). Graphene coated cotton fabric as textile structured counter electrode for DSSC. *Electrochimica Acta*, *173*, 164-171.
49. Shateri-Khalilabad, M., & Yazdanshenas, M. E. (2013). Preparation of superhydrophobic electroconductive graphene-coated cotton cellulose. *Cellulose*, *20*(2), 963-972.
50. Kaushik, V., Lee, J., Hong, J., Lee, S., Lee, S., Seo, J., & Lee, T. (2015). Textile-based electronic components for energy applications: principles, problems, and perspective. *Nanomaterials*, *5*(3), 1493-1531.
51. Lin, Zhaoyang, Courtney Hollar, Joon Sang Kang, Anxiang Yin, Yiliu Wang, Hui-Ying Shiu, Yu Huang, Yongjie Hu, Yanliang Zhang, and Xiangfeng Duan. "A Solution Processable High-Performance Thermoelectric Copper Selenide Thin Film." *Advanced Materials* 29, no. 21 (2017): 1606662.
52. https://www.astm.org/Standards/textile-standards.html
53. Khoso, N. A., Ahmed, A., Deb, H., Tian, S., Jiao, X., Gong, X. Y., & Wang, J. (2019). Controlled template-free in-situ polymerization of PEDOT for enhanced thermoelectric performance on textile substrate. *Organic Electronics*, *75*, 105368.
54. Kim, M. K., Kim, M. S., Lee, S., Kim, C., & Kim, Y. J. (2014). Wearable thermoelectric generator for harvesting human body heat energy. *Smart Materials and Structures*, *23*(10), 105002.
55. Lee, S. H., Park, H., Son, W., Choi, H. H., & Kim, J. H. (2014). Novel solution-processable, dedoped semiconductors for application in thermoelectric devices. *Journal of Materials Chemistry A*, *2*(33), 13380-13387.
56. Liu, H., Wang, Y., Mei, D., Shi, Y., & Chen, Z. (2017). Design of a wearable thermoelectric generator for harvesting human body energy. In *Wearable sensors and robots* (pp. 55-66). Springer, Singapore.